ISSN 1068-3755, Surface Engineering and Applied Electrochemistry, 2023, Vol. 59, No. 5, pp. 649–660. © Allerton Press, Inc., 2023.
Russian Text © The Author(s), 2023, published in Elektronnaya Obrabotka Materialov, 2023, No. 3, pp. 20–31.

Study of the Characteristics and Parameters of Plasma of Overvoltage Nanosecond Discharge in Krypton between the Electrodes of a Superionic Conductor—Silver Sulphide

A. K. Shuaibov[a], *, A. I. Minya[a], R. V. Gritsak[a], A. N. Malinin[a], A. A. Malinina[a], R. M. Golomb[a], and Z. T. Gomoki[a]

[a] *Uzhgorod National University, Uzhgorod, 88000 Ukraine*

**e-mail: alexsander.shuaibov@uzhnu.edu.ua*

Received November 19, 2022; revised May 17, 2023; accepted May 24, 2023

Abstract—The results of a study into the electrical and optical characteristics of an overvoltage nanosecond atmospheric pressure discharge between electrodes made of a superionic conductor (SIC) (Ag_2S) in krypton are presented. The destruction of electrodes in the discharge and the introduction of Ag_2S vapor into the interelectrode gap occurred due to the microexplosions of inhomogeneities on the working surfaces of polycrystalline electrodes (the formation of ectons) in order to synthesize thin films based on this compound on the surface of a dielectric substrate mounted near the electrodes. Numerically solving the Boltzmann kinetic equation for the electron energy distribution function, the temperature and the electron density in the discharge, the specific discharge power losses for the main electronic processes, and the rate constants of the electronic processes depending on the parameter E/N for the plasma of vapor-gas mixtures based on krypton and silver sulfide have been calculated. Homogeneous thin films based on silver sulfide are synthesized on the quartz substrates by the gas-discharge method under conditions of ultraviolet assisted discharge plasma.

Keywords: overvoltage nanosecond atmospheric pressure discharge, plasma, krypton, thin films, silver sulfide, radiation

DOI: 10.3103/S1068375523050162

INTRODUCTION

An overview of the current state of the development of ion sources based on superionic conductors (SICs) for aerospace technologies and ion-beam technologies is provided in [1]. The methods of synthesis and properties of hard electrolytes, formation of mobile ions, and rapid ion transport in the thin electrolyte film under the action of an external electrical field, as well as the processes of ion emission from the electrolyte surface into vacuum, have been considered. The operation modes, design, and technology of manufacturing the anion and cation sources are presented, and methods to improve the performance and the main areas of application are analyzed.

In the chemical synthesis of silver compounds with halogen atoms, mainly microscopic specimens in the form of polycrystals are received, though the vast majority of their applications in power electronics (capacitors, accumulators, etc.) need specimens in the form of thin films. Therefore, it is now relevant to search and optimize new physical methods of synthesis of film micro- and nanostructures based on silver compounds with chalcogens such as Ag_2S, Ag_2Se, etc.

The application of the overvoltage nanosecond discharge between the electrodes of transition metals (Cu, Zn, Al ...) in air or in oxygen made it possible to synthesize thin films based on the oxides of these metals [2, 3]. Similar experiments with the overvoltage nanosecond discharge between the electrodes of triple chalcopyrite ($CuInSe_2$) and the electrode of aluminum and triple chalcopyrite in different atmospheric pressure gases have provided the opportunity to synthesize films of $CuInSe_2$ and $CuAlInSe_2$ [4, 5]. Under these conditions, the ecton mechanism of spraying the electrode material [6] is achieved when, in a strong electric field of gas discharge, the microexplosions of natural points occur on the electrode surfaces and their material is introduced into plasma. The synthesis of thin films of the electrode material is possible on the substrate of dielectric mounted at the system of electrodes. If the plasma of these discharges intensively radiate ultraviolet light, then assisting to the synthesis of the films with ultraviolet allows a positive impact on the surface nanostructures, in particular, reducing their resistance [7]. The plasma on the basis of silver is characterized by intensive spectral lines of Ag I and Ag II; therefore, the application of the overvoltage nano-

second discharge between the electrodes of silver sulphide (Ag_2S) can appear promising.

Our previous experiments concerning the synthesis of thin films based on the compound Ag_2S in the medium of atmospheric pressure inert gases showed that, when helium and neon are applied, the synthesized film is very heterogeneous: a film of silver is deposited in the center, and other Ag_2S compounds of different destruction products are deposited round it. A high energy of discharge electrons or a high energy of metastable atoms He(m) and Ne(m) in the plasma based on light inert gases is a possible reason for the destruction of the initial compound of the material of the electrodes of Ag_2S or other similar compounds in this discharge. Therefore, in these experiments, krypton is chosen as a buffer gas.

At present no conditions for the synthesis of thin films based on the Ag_2S SIC using the nanosecond overvoltage discharge between the electrodes of silver sulphide in atmospheric pressure krypton are established.

The study results for the electric and spectral characteristics of the overvoltage nanosecond discharge in the atmospheric pressure krypton between the polycrystalline electrodes of SIC (Ag_2S), the output of simulation of plasma parameters in the silver sulphide vapor–krypton mixture, and the indicators of the spectra of the Raman scattering of laser radiation at a wavelength of 785 nm by thin films synthesized from the electrode erosion products are presented in the article.

EXPERIMENTAL TECHNIQUES AND CONDITIONS

The atmospheric pressure overvoltage nanosecond discharge in krypton between the electrodes of polycrystalline SIC based on the compound Ag_2S was ignited in the discharge chamber made of plexiglass. Its design is presented in [8]. The massive specimens of polycrystals based on the Ag_2S SIC were synthesized in the technological laboratory of chemistry department at Uzhgorod National University.

The ignition of the overvoltage nanosecond discharge occurred with the help of a high-voltage modulator of bipolar pulses of voltage with a total duration of 50–150 ns and the total amplitude of positive and negative compounds ±20–60 kV. The generator of high-voltage nanosecond pulses is constructed according to the scheme with a resonance recharging of the accumulating low-inductive condenser with a capacity of 1540 pF. A hydrogen pulse thyratron TGII-1000-25 served as a commutator in the modulator. The voltage pulse repetition frequency can be varied in the range 40–1000 Hz.

The pulse electric power of the overvoltage nanosecond discharge was determined by graphic multiplication of the oscillograms of the voltage and current pulses. Time integration of the pulse power made it possible to receive an energy in one electric pulse introduced into plasma.

The overvoltage nanosecond discharge was ignited at a distance between the electrodes of 2 mm. The working end parts of the electrodes had a rounding radius of about 10 mm. The radius of cylinder electrodes was 5 mm.

The oscillograms of voltage pulses over the discharge gap and the oscillograms of the current pulses were recorded with a wideband capacitive voltage divider, a Rogowski toroidal coil, and a 6LOR-04 high-bandwidth oscilloscope. The temporal resolution of this system to measure the electric pulse characteristics was 2–3 ns.

The digital two-channel spectrometer with the compensation of astigmatism SL-40-2-1024USB was used to record the plasma emission spectra. The working spectrum of the spectrometer was 200–1200 nm.

The experimental techniques was described in [8] in more detail.

The nanosecond discharge was ignited at the overvoltage of the discharge gap when a beam of the runaway electrons was formed in it [9]. Under the effect of this beam, collateral X-ray radiation, and the impurity of easily ionized material (Ag_2S compound), the discharge in the atmospheric pressure krypton was sufficiently homogeneous even at rather heterogeneous distribution of the electric field strength between the electrodes with the rounding radii of the hemispherical working surfaces (Fig. 1). The microexplosions of nanowhiskers occur in the strong electric field on the working surface of the electrode based on the Ag_2S SIC [7], which contributes to the introduction of vapors of the Ag_2S SIC and the decomposition products (Ag, Ag^+, S ...) into plasma and further deposition of them on the glass substrate in the form of a thin film.

When the quartz substrate was mounted at a distance of 2–4 cm from the discharge gap center and at a discharge burning time of 30 min, a thin film of the scattering products of the electrode material was deposited on the substrate.

The pictures of discharge were taken using the digital camera (exposition time ≈1 s). The pictures of the thin film surface were reproduced with the help of an optical microscope and camera with an increase of the system of 1500.

CHARACTERISTICS OF DISCHARGE AND SYNTHESIZED FILMS

The oscillograms of current pulses, voltage, and pulse power of the overvoltage nanosecond discharge between the electrodes of the Ag_2S compound in kryp-

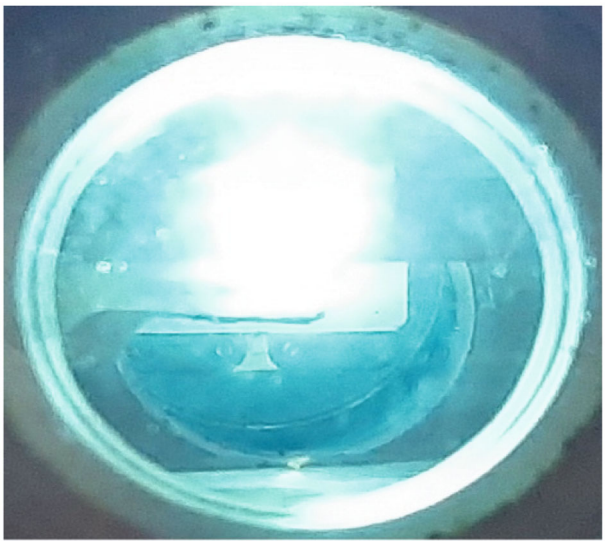

Fig. 1. Picture of overvoltage nanosecond discharge between polycrystalline electrodes of compound Ag_2S in krypton at p = 101 kPa and f = 1 kHz.

ton and the energy contribution to plasma in a single pulse are presented in Fig. 2.

In this experiment the total duration of voltage pulses could be as high as 400–450 ns, and the voltage pulse itself consisted of decaying with time oscillations with a duration of about 40–50 ns. The maximum value of voltage drop over the discharge gap was 20–27 kV, taking into account the positive and negative components of voltage pulse. The maximum amplitude of the current pulse was 150–250 A. The highest value of the discharge pulse power was achieved during the initial 100 ns from the moment of its ignition, and it was about 10 MW (at t = 50–70 ns). The second maximum of the pulse power was 8 MW at the time moment t = 70–100 ns from the start of discharge ignition. The energy of a single pulse grew from 37.3 to 630.8 mJ with an increase in the charge voltage from 13 to 20 kV. The radiation spectrum of plasma of the overvoltage nanosecond discharge in krypton based on the SIC and the identification results for the most intense spectral lines of the atoms of sulfur, silver, krypton, and the one-charge ions of sulfur and silver in the discharge are presented in Fig. 3 and Table 1.

The decrease in the intensity of spectral lines of silver upon the reduction in the discharge pulse repetition frequency is caused by the decrease in the concentration of the electrode material and its decomposition products in the discharge plasma. It may also be noted that the reduction in the frequency by 12.5 times leads to the different decrease in the intensity of different lines. This may indicate a complex nature of the formation of components, conditions of their excitation, and radiation. Handbooks [10, 11] were used to identify the spectral lines of the discharge plasma radiation spectrum. As Table 1 shows, the studied plasma radiates intensely in the spectral range 200–340 nm. The main sources of radiation within the shortwave spectral range 200–300 nm were one-charge ions of silver, and in the spectral interval 300–340 nm they were the atoms of silver.

The dynamics of plasma radiation of the main excited components is presented in Table 2. The maximum of the discharge current 82 A in value was achieved at a time moment of 52 ns. As Fig. 4 shows, most of the radiation of atoms and ions was observed in the discharge afterglow, i.e., after the maximum current was achieved.

In powerful atmospheric pressure pulse discharges with electron density of about 10^{15}–10^{17} cm^{-3}, the for-

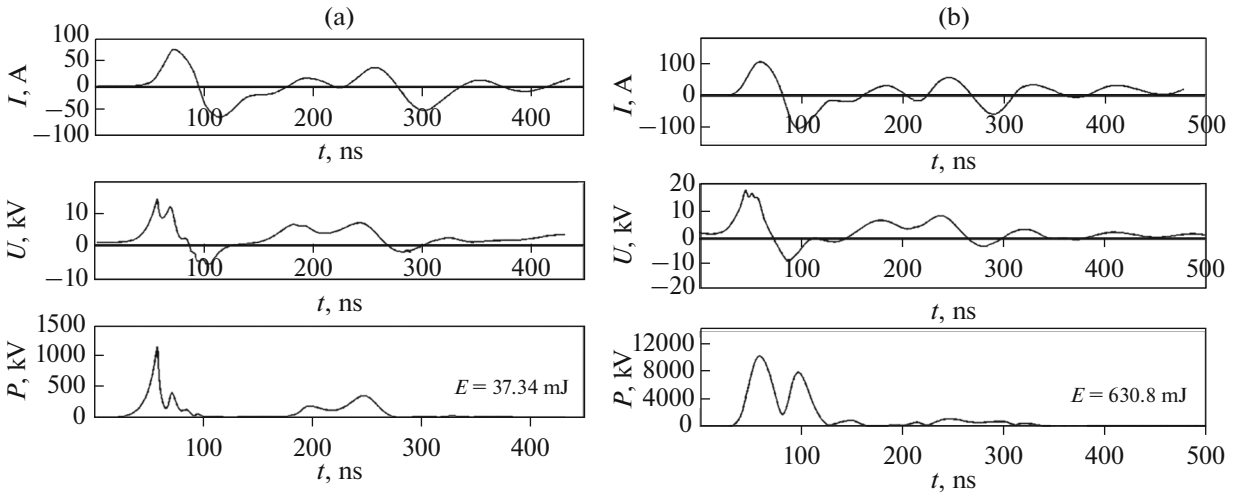

Fig. 2. Oscillograms of pulses of current I, voltage U, and pulse power P of overvoltage nanosecond discharge in krypton at pressure p = 101 kPa, interelectrode distance d = 2 mm and f = 1 kHz, and magnitude of charge voltage of working capacitor of high-voltage modulator U = 13 (a) and 20 (b) kV.

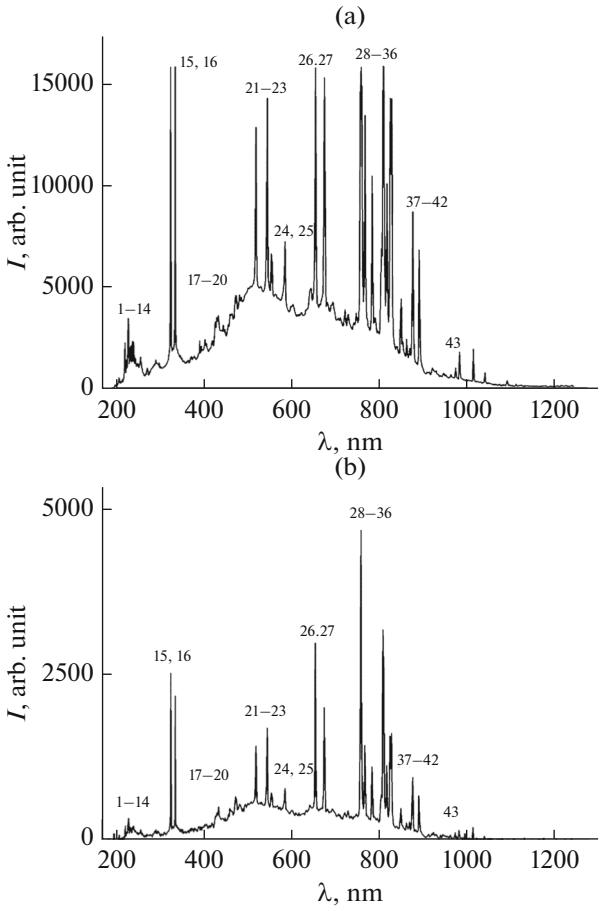

Fig. 3. Radiation spectra of overvoltage nanosecond discharge between electrodes of SIC in krypton (p = 101 kPa) at frequency f =1 (a) and 0.08 (b) kHz.

mation of excited ions of metals occurred mainly in the processes of their excitation by the electrons typical for the atoms of copper and aluminum [8]. These effects in the behavior of the intensity of the spectral lines of silver were also observed in the nanosecond overvoltage charge between the electrodes of Ag_2S in the atmospheric pressure air [12]. The pictures of the surface of the thin films that formed based on the compound Ag_2S (Fig. 5), taken with the help of an optical microscope, showed that they were uniform enough. Only individual heterogeneities of some micrometers were seen in them, which could be caused by the destruction of the polycrystalline electrodes in the overvoltage nanosecond discharge. To improve the homogeneity of the synthesized films and reduce the time of their synthesis, it is necessary to weaken the energy in the electric pulse, which can be reached decreasing the duration of the energy contribution to the plasma and increasing the pulse repetition frequency.

PLASMA PARAMETERS

The discharge plasma parameters for the mixtures of Ag_2S and krypton vapors at atmospheric pressure (proportion of components 200 Pa: 101.3 kPa and 1000 Pa: 101.3 kPa) were determined numerically and calculated as full integrals of the function of the electron energy distribution (FEED) in the discharge. The FEEF was calculated numerically solving the Boltzmann kinetic equation at the two-member approximation. The calculation of the FEED was carried out using the program described in [13]. On the basis of the received FEED for electrons, the following were determined: average energies, temperatures, drift rates, concentrations, and constants of the excitation rates of the silver atom levels. This allowed us to determine the specific losses of the discharge for elastic and inelastic processes of collision of electrons with atoms and ions of both mixtures, depending on the magnitude of the reduced electric field (the ratio between the electric field E and the general concentration N of the mixture of krypton atoms and Ag_2S molecules—E/N). The range of the parameter variation was E/N = 1–1000 Td (1×10^{-17}– 1×10^{-14} V cm^2) and included the quantities of E/N realized in the experiment. These electric field values were 306 and 102 Td, and also 304 and 101 Td for times 50–100 ns of the voltage pulses (Fig. 2) from the start of discharge burning. In the integral of electron collisions with atoms and molecules, the following processes are taken into account: the elastic scattering of electrons on silver atoms, the excitation of the levels of silver atoms and ions (threshold energies 6.01, 3.78, 3.66, 7.19, 7.02, 6.71, 5.99, and 17 eV)), the ionization of silver atoms (threshold energy of 8.00 eV); the elastic scattering of electrons on krypton atoms, the excitation of levels of krypton atoms (threshold energies 9.91, 10.03, 10.56, 10.64, and 11.30 eV), and the ionization of krypton atoms (threshold energy 14.00 eV).

Data concerning the absolute values of the effective cross sections of these processes, as well as their dependences on the electron energies, are taken from the databases of these articles [14], [15].

Figure 6 presents the dependencies of the average energy of electrons in plasma of the gas–vapor mixture Ag_2S–Kr = 200 : 101 300 Pa (I) and Ag_2S–Kr = 1000 : 101 300 Pa (II) on E/N at the general pressure p = 101 500 Pa and 102 300 Pa, respectively.

The average energy of the discharge electrons for the silver sulphide–krypton vapor–gas mixtures nearly linearly increases from 1.45 to 13.21 eV (Fig. 6) (curve *1*) and from 1.257 to 12.87 (curve *2*) when E/N grows from 1 to 1000 Td with the regularity of the increased rate of its change in the range 1–50 Td for the first and second mixtures. For the range of E/N from 101 to 306 Td at which the experimental investigation of the electric and optical characteristics of the discharge were carried out, the average energies of electrons were changed in the range 5.409–7.213 eV

Table 1. Results of identifying the most intense spectral lines of radiation of Ag_2S–Kr mixture components of overvoltage nanosecond discharge plasma at pressure $p = 101$ kPa, interelectrode distance $d = 2$ mm, charge voltage value $U = 20$ kV, and pulse repetition frequency $f = 1$ kHz (energies of lower E_{low} and upper E_{up} levels with therms $Therm_{low}$ and $Therm_{up}$)

No.	λ_{table}, nm	I_{exp}, arb. unit	Object	E_{low}, eV	E_{up}, eV	$Therm_{low}$	$Therm_{up}$
1	211.38	517	Ag II	4.85	10.71	$4d^9(^2D_{5/2})5s\ ^2[^5/_2]_3$	$4d^9(^2D_{5/2})5p\ ^2[^5/_2]^\circ_3$
2	224.64	2248	Ag II	4.85	10.37	$4d^9(^2D_{5/2})5s\ ^2[^5/_2]_3$	$4d^9(^2D_{5/2})5p\ ^2[^7/_2]^\circ_4$
3	227.99	1142	Ag II	5.70	11.05	$4d^9(^2D_{3/2})5s\ ^2[^3/_2]_2$	$4d^9(^2D_{3/2})5p\ ^2[^5/_2]^\circ_3$
4	232.02	2680	Ag II	5.05	10.36	$4d9(^2D_{5/2})\ 5s\ ^2[^5/_2]_2$	$4d^9(^2D_{5/2})\ 5p\ ^2[^3/_2]]^\circ_1$
5	233.13	3458	Ag II	5.05	10.36	$4d^9(^2D_{5/2})5s\ ^2[^5/_2]_2$	$4d^9(^2D_{5/2})5p\ ^2[^3/_2]^\circ_1$
6	241.13	1313	Ag II	5.42	10.56	$4d^9(^2D_{3/2})5s\ ^2[^3/_2]_1$	$4d^9(^2D_{5/2})5p\ ^2[^5/_2]_2$
7	243.77	2320	Ag II	4.85	9.94	$4d^9(^2D_{5/2})5s\ ^2[^5/_2]_3$	$4d^9(^2D_{5/2})5p\ ^2[^3/_2]^\circ_2$
8	244.78	2292	Ag II	5.70	10.77	$4d^9(^2D_{3/2})5s\ ^2[^3/_2]_2$	$4d^9(^2D_{3/2})5p\ ^2[^5/_2]_2$
9	260.59	1298	Ag II	10.18	14.94	$4d^9(^2D_{5/2})5p\ ^2[^7/_2]^\circ_3$	$4d^9(^2D_{5/2})6s\ ^2[^5/_2]_3$
10	261.43	1542	Ag II	10.77	15.51	$4d^9(^2D_{3/2})5p\ ^2[^5/_2]^\circ_2$	$4d^9(^2D_{3/2})6s\ ^2[^3/_2]_1$
11	266.04	769	Ag II	12.14	16.78	$4d^85s^2\ ^3F_3$	$4d^8(^3F)5s5p(^3P^\circ)^5G^\circ_2$
12	271.17	715	Ag II	10.37	14.94	$4d^9(^2D_{5/2})\ 5p\ ^2[^7/_2]^\circ_4$	$4d^9(^2D_{5/2})\ 6s\ ^2[^5/_2]_3$
13	276.75	1008	Ag II	5.70	10.18	$4d^9(^2D_{3/2})5s\ ^2[^3/_2]_2$	$4d^9(^2D_{5/2})5p\ ^2[^7/_2]^\circ_3$
14	293.83	1291	Ag II	10.77	14.99	$4d^9(^2D_{3/2})5p\ ^2[^5/_2]^\circ_2$	$4d^9(^2D_{5/2})6s\ ^2[^5/_2]_2$
15	328.06	15867	Ag I	0.00	3.77	$4d^{10}5s\ ^2S_{1/2}$	$4d^{10}5p\ ^2P^\circ_{3/2}$
16	338.28	15887	Ag I	0.00	3.66	$4d^{10}5s\ ^2S_{1/2}$	$4d^{10}5p\ ^2P^\circ_{1/2}$
17	405.54	2146	Ag I	3.66	6.72	$4d^{10}5p\ ^2P^\circ_{1/2}$	$4d^{10}6d\ ^2D_{3/2}$
18	424.06	2349	Ag II	14.08	17.00	$4d^85s^2\ ^1G_4$	$4d^9(^2D_{3/2})6p\ ^2[^5/_2]^\circ_3$
19	435.54	3295	Kr II	13.98	16.83	$4s^24p^4(^3P)5s\ ^4P_{5/2}$	$4s^24p^4(^3P)5p\ ^4D^\circ_{7/2}$
20	490.24	4502	S II	15.55	18.08	$3s^23p^2(^3P)4p\ ^2S^\circ_{1/2}$	$3s3p^4\ ^2P_{1/2}$
21	520.90	12889	Ag I	3.66	6.04	$4d^{10}5p\ ^2P^\circ_{1/2}$	$4d^{10}5d\ ^2D_{3/2}$
22	531.24	5001	Ag II	15.70	18.03	$4d^9(^2D_{5/2})5d\ ^2[^9/_2]_4$	$4d^9(^2D_{5/2})\ 4f\ ^2[^9/_2]^\circ_4$
23	547.86	14339	Ag II	15.71	17.97	$4d^9(^2D_{5/2})5d\ ^2[^3/_2]_2$	$4d^9(^2D_{5/2})4f\ ^2[1/2]^\circ_1$
24	557.02	6639	Kr I	9.91	12.14	$4s^24p^5(^2P^\circ_{3/2})5s\ ^2[^3/2]^\circ_2$	$4s^24p^5(^2P^\circ_{1/2})5p\ ^2[^1/_2]_1$
25	587.09	7243	Kr I	10.03	12.14	$4s^24p^5(^2P^\circ_{3/2})5s\ ^2[^3/2]^\circ_1$	$4s^24p^5(^2P^\circ{}_{1/2})5p\ ^2[^3/_2]_2$
26	657.07 −328.06 (2)	15841	Ag I	0.00	3.77	$4d^{10}5s\ ^2S_{1/2}$	$4d^{10}5p\ ^2P^\circ_{3/2}$

Table 1. (Contd.)

No.	λ_{table}, nm	I_{exp}, arb. unit	Object	E_{low}, eV	E_{up}, eV	$Therm_{low}$	$Therm_{up}$
27	679.2 −338.28 (2)	15341	Ag I	0.00	3.66	$4d^{10}5s\ ^2S_{1/2}$	$4d^{10}5p\ ^2P^\circ_{1/2}$
28	760.15	15861	Kr I	9.91	11.54	$4s^24p^5(^2P^\circ_{3/2})5s\ ^2[^3/_2]^\circ_2$	$4s^24p^5(^2P^\circ_{3/2})5p\ ^2[^3/_2]_2$
29	769.45	13488	Kr I	9.91	11.52	$4s^24p^5(^2P^\circ_{3/2})5s\ ^2[^3/_2]^\circ_2$	$4s^24p^5(^2P^\circ_{3/2})5p\ ^2[^3/_2]_1$
30	785.48	10490	Kr I	10.56	12.14	$4s^24p^5(^2P^\circ_{1/2})5s\ ^2[^1/_2]^\circ_0$	$4s^24p^5(^2P^\circ_{1/2})5p\ ^2[^1/_2]_1$
31	800.51	2855	Ag II	14.94	16.49	$4d^9(^2D_{5/2})6s\ ^2[^5/_2]_3$	$4d^9(^2D_{5/2})\ 6p\ ^2[^5/_2]^\circ_3$
32	810.43	15915	Kr I	9.91	11.44	$4s^24p^5(^2P^\circ_{3/2})5s\ ^2[^3/_2]^\circ_2$	$4s^24p^5(^2P^\circ_{3/2})5p\ ^2[^5/_2]_2$
33	819.00	10110	Kr I	10.03	11.54	$4s^24p^5(^2P^\circ_{3/2})5s\ ^2[^3/_2]^\circ_1$	$4s^24p^5(^2P^\circ_{3/2})5p\ ^2[^3/_2]_2$
34	826.32	14340	Kr I	10.64	12.14	$4s^24p^5(^2P^\circ_{1/2})5s\ ^2[^1/_2]^\circ_1$	$4s^24p^5(^2P^\circ_{1/2})5p\ ^2[^3/_2]_2$
35	829.81	14317	Kr I	10.03	11.52	$4s^24p^5(^2P^\circ_{3/2})5s\ ^2[^3/_2]^\circ_1$	$4s^24p^5(^2P^\circ_{3/2})5p\ ^2[^3/_2]_1$
36	841.24	2064	Kr I	11.54	13.01	$4s^24p^5(^2P^\circ_{3/2})5p\ ^2[^3/_2]_2$	$4s^24p^5(^2P^\circ_{3/2})5d\ ^2[^3/_2]^\circ_2$
37	850.88	3177	Kr I	10.64	12.10	$4s^24p^5(^2P^\circ_{1/2})5s\ ^2[^1/_2]^\circ_1$	$4s^24p^5(^2P^\circ_{1/2})5p\ ^2[^3/_2]_1$
38	869.47	1680	S I	7.86	9.29	$3s^23p^3\ (^4S^\circ)4p\ ^5P_3$	$3s^23p^3(^4S^\circ)4d\ 5D^\circ_4$
39	877.67	8719	Kr I	10.03	11.44	$4s^24p^5(^2P^\circ_{3/2})5s\ ^2[^3/_2]^\circ_1$	$4s^24p^5(^2P^\circ_{3/2})5p\ ^2[^5/_2]_2$
40	892.86	6841	Kr I	9.91	11.30	$4s^24p^5(^2P^\circ_{3/2})5s\ ^2[^3/_2]^\circ_2$	$4s^24p^5(^2P^\circ_{3/2})5p\ ^2[^1/_2]_1$
41	942.19	605	S I	8.40	9.72	$3s^23p^3(^2D^\circ)4s\ ^3D^\circ_2$	$3s^23p^3(^2D^\circ)4p\ ^3F_3$
42	964.95	680	S I	8.41	9.69	$3s^23p^3(^2D^\circ)4s\ ^3D^\circ_3$	$3s^23p^3(^2D^\circ)4p\ ^3D_3$
43	975.17	1008	Kr I	10.03	11.30	$4s^24p^5(^2P^\circ_{3/2})5s\ ^2[^3/_2]^\circ_1$	$4s^24p^5(^2P^\circ_{3/2})5p\ ^2[^1/_2]_1$

Table 2. Radiation of most intense spectral lines Ag II, Ag I, and Kr II

λ_{table}, nm	Object	Maximum glow intensity, arb. unit	Glow time moment, ns
276.75	Ag II	64	106
293.83	Ag II	37	85
424.06	Ag II	110	101
328.06	Ag I	94	106
338.28	Ag I	70	102
405.54	Ag I	111	103
435.5	Kr II	90	113

for the mixture with a lower partial pressure of 5.409–7.213 (Fig. 6, curve *1*) and 4.789–6.832 for the mixture with their higher partial pressure (Fig. 6, curve 2).

The calculation results for the transport characteristics of electrons are presented in Table 3: the average energies ε, the temperature *T,* the drift rate V_{dr}, and the concentration of electrons for two mixtures of Ag_2S vapors with krypton.

The temperature and the drift rates of electrons (Table 2) decrease from 83671 to 62 744 K and from 2.2×10^5 to 8.2×10^4 m/s for the first mixture and from 62 744 to 55552 K and 2.2×10^5 to 8.8×10^4 for the second mixture in the case of changing E/N from 306 to 101 Td, respectively. The values of the electron concentration increase from 7.2×10^{19} to 3.89×10^{20}

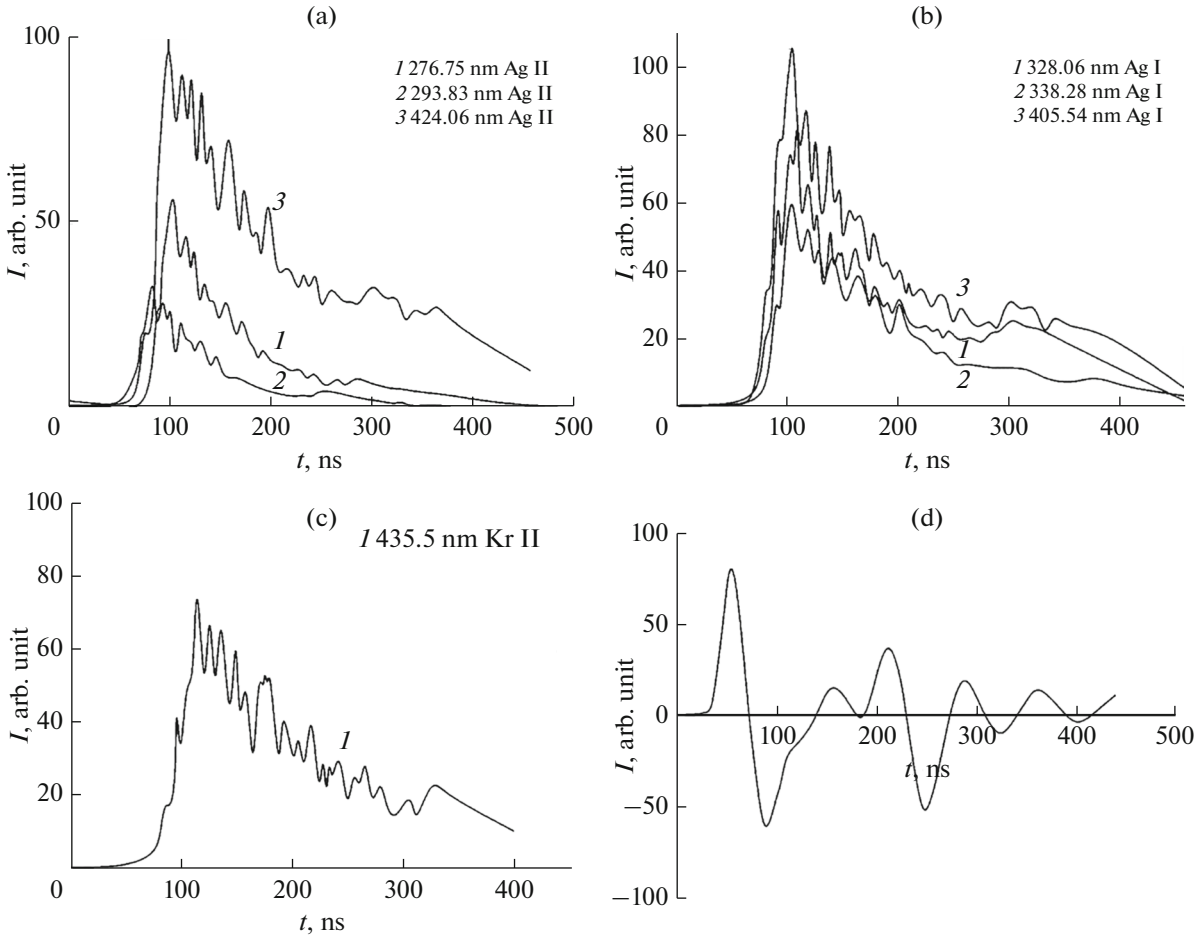

Fig. 4. Oscillograms of radiation of most intense spectral lines Ag II, Ag I, and Kr II (a–c) and oscillogram of current of overvoltage nanosecond discharge between electrodes of Ag_2S (d) at interelectrode distance of 2 mm and atmospheric pressure of krypton.

m^{-3} for the first mixture and from 7.2×10^{19} to 3.6×10^{20} m^{-3} for the second mixture.

Figure 7 presents the specific powers of the discharge losses at the elastic and inelastic processes of electron collisions with the mixture components in the gas-discharge plasma versus E/N. The power at the growing values of E/N both for the elastic processes and the inelastic processes is increased. In addition, higher values of the specific powers of the discharge losses for the elastic (in the mixture I = 200 : 101

Table 3. Transport characteristics of electrons for mixtures: Ag_2S–Kr = 200–101 300 Pa (I) and Ag_2S– Kr = 1000–101 300 Pa (II)

τ, ns	E/N, Td	Mixture: I = 200–101 300 Pa			
		ε, eV	T, K	V_{dr}, m/s	N_e, m^{-3}
50	306	7.213	83671	2.2×10^5	7.2×10^{19}
100	102	5.409	62744	8.2×10^4	3.89×10^{20}
τ, ns	E/N, Td	Mixture II = 1000–101 300 Pa			
		ε, eV	T, K	V_{dr}, m/s	N_e, m^{-3}
50	304	6.832	62744	2.2×10^5	7.2×10^{19}
100	101	4.789	55552	8.8×10^4	3.6×10^{20}

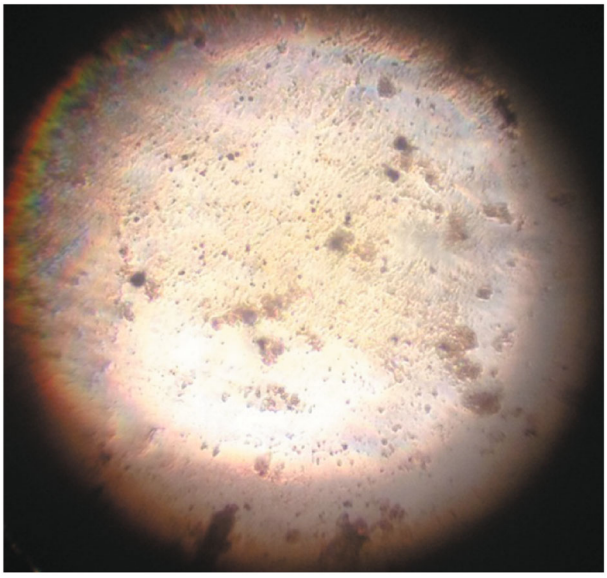

Fig. 5. Picture of surface area of thin film synthesized from destruction products of polycrystalline electrodes based on Ag_2S SIC in overvoltage nanosecond discharge in krypton at pressure 101 kPa and frequency 1 kHz.

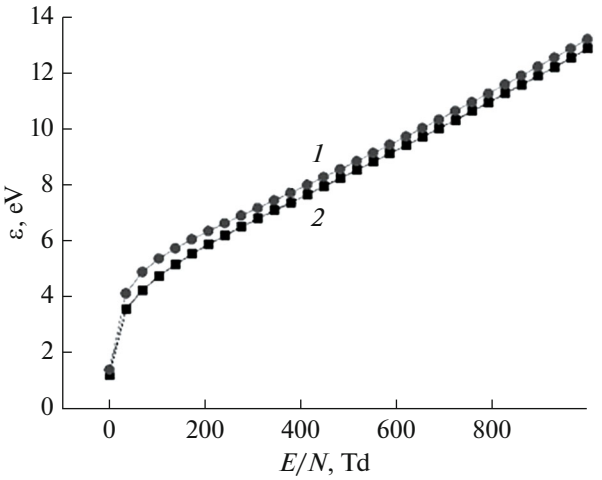

Fig. 6. Average energy of electrons in plasma of vapor–gas mixture versus E/N: (*1*) Ag_2S–Kr = 200 : 101 300 Pa; (*2*) Ag_2S–Kr = 1000 : 101 300 Pa at total pressure p = 101 500 (*1*) and 102 300 Pa (*2*).

300 Pa) and inelastic processes of electron collisions with the mixture components (in the mixture II = 1000 : 101 300 Pa (Fig. 7, Table 4)) are noted.

The specific losses of the discharge power in the mixtures Ag_2S–Kr = 200–101 300 Pa (Fig. 8a) and Kr–Ag_2S = 101 300 : 1000 Pa (Fig. 8b) at the inelastic processes of electron collisions with silver atoms (Fig. 7, curve *2*) achieved the values of 82% for the second mixture (Fig. 7b) and 55% for the first mixture (Fig. 7a) at E/N = 35 Td. For the mixture Ag_2S–Kr = 1000–101 300 Pa (Fig. 7b), they were nearly twice as large as for the mixture Ag_2S–Kr = 200–101 300 Pa (Fig. 7a). At the excitation of the line of silver atoms with a wavelength of λ = 328.068 nm (Fig. 7b, curve *3* at E/N = 1 Td), they reached a value of 42%. The rate of growth and drop of the discharge power losses for the processes of the excitation of electron states and the ionization and their values are connected with the nature of the dependence of the effective cross sections of the inelastic processes of electron collisions with the working medium components on the electron energy and their absolute values, as well as with the dependence of the electron distribution function on E/N and the threshold energies of the processes [16].

Figure 9 and Table 5 present the numerical calculation results for the dependence of the excitation rate constants for the spectral lines of silver atoms on E/N

Table 4. Elastic and inelastic losses of specific power for mixtures Ag_2S–Kr

Specific power of losses (eV m^3/s) in processes of collisions with electrons		
Mixture I = 200–101 300 Pa		
E/N, Td	Elastic (10^{-16})	Inelastic (10^{-14})
306	0.2226	5.935
102	0.1519	0.8370
Mixture II = 1000–101 300 Pa		
E/N, Td	Elastic (10^{-16})	Inelastic (10^{-14})
304	0.2089	6.220
101	0.1246	0.9295

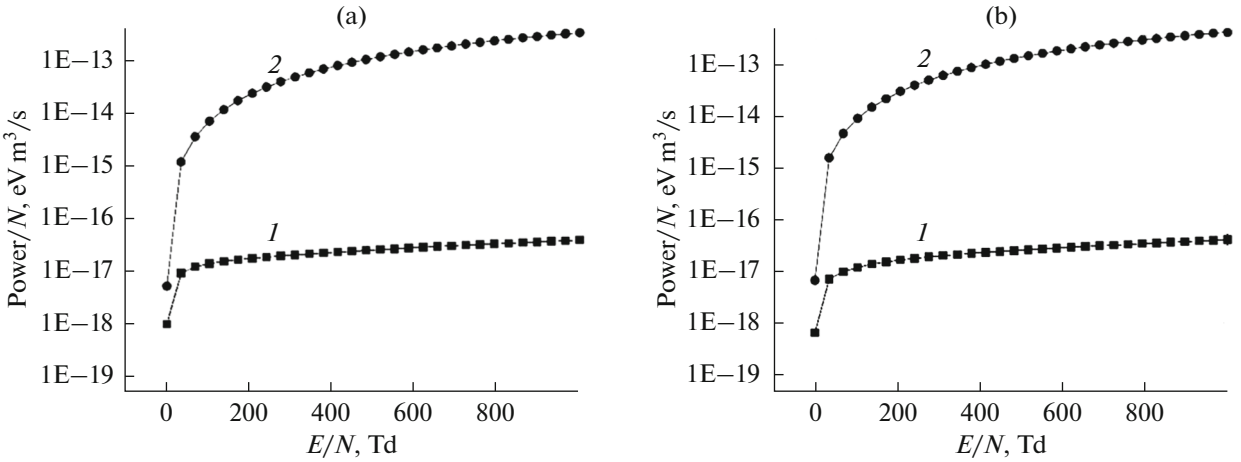

Fig. 7. Specific power of discharge consumed for elastic (*1*) and inelastic (*2*) processes per general concentration unit versus E/N for mixtures: Ag_2S–Kr = 200 : 101 300 Pa (a) and Ag_2S–Kr = 1000 : 101 300 Pa (b).

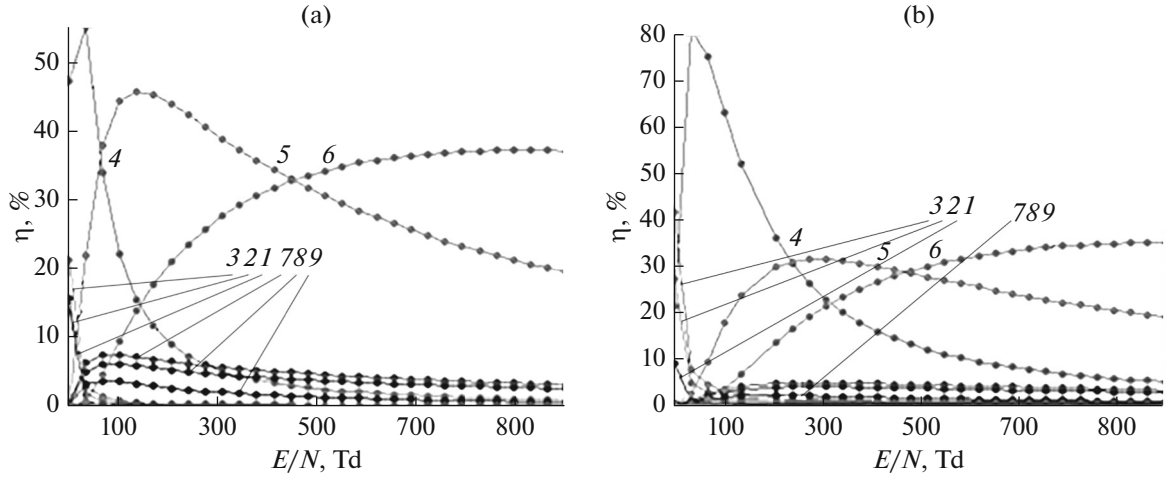

Fig. 8. Specific losses of discharge power consumed for processes of collision of electrodes with atoms of silver and krypton versus E/N in plasma for mixtures Ag_2S–Kr = 200 : 101 300 Pa (a) and Ag_2S–Kr = 1000 : 101 300 Pa (b): (*1*) elastic scattering of electrons on krypton atoms, (*2*) excitation of silver atom level (E_{thr} = 3.66 eV, λ = 338.289 nm), (*3*) excitation of silver atom level (E_{thr} = 3.78 eV, λ = 328.068 nm), (*4*) total inelastic scattering (excitation and ionization) of electrons on silver atoms, (*5*) excitation of krypton atom level (E_{thr} = 11.30 eV, λ = 892.86 nm), (*6*) ionization of krypton atoms (E_{thr} = 14.00 eV), (*7*) excitation of krypton atom level (E_{thr} = 10.03 eV), (*8*) excitation of krypton atom level (E_{thr} = 10.64 eV), and (*9*) excitation of krypton atom level (E_{thr} = 11.30 eV, λ = 975.17 nm).

in the vapor mixtures of Ag_2S and krypton for the ratio of partial pressures in the mixtures 200–101 300 Pa (Fig. 9a) and 1000–101 300 Pa (Fig. 9b).

The excitation rate constants are characterized by a high value that is associated with the value of the absolute effective cross sections of the corresponding processes [16]. In the range of E/N from 306 to 101 Td of the experimental studies of the electric and optical characteristics of the discharge, they were within the value range $k \approx 0.6 \times 10^{-20} - 0.2 \times 10^{-13}$ m^3/s [17]. The maximum value of the constant of the excitation rate of the resonant spectral line λ = 328.06 nm of the silver atoms was 0.2098×10^{-13} for E/N being 306 Td.

OPTICAL CHARACTERISTICS OF THIN FILMS

If a substrate of glass is mounted at a distance of 2–4 cm from the center of the discharge gap and the pulse repetition frequency is from 500 to 1000 Hz, sufficiently homogeneous thin films are synthesized of the erosion products of the electrodes of the overvoltage nanosecond discharge in heavy inert gases (Kr, Ar). The optical characteristics of films synthesized in krypton or argon were almost the same. The pressure of inert gases was 101 kPa. In the process of the synthesis of films, they were always under the action of the ultraviolet radiation of the discharge plasma.

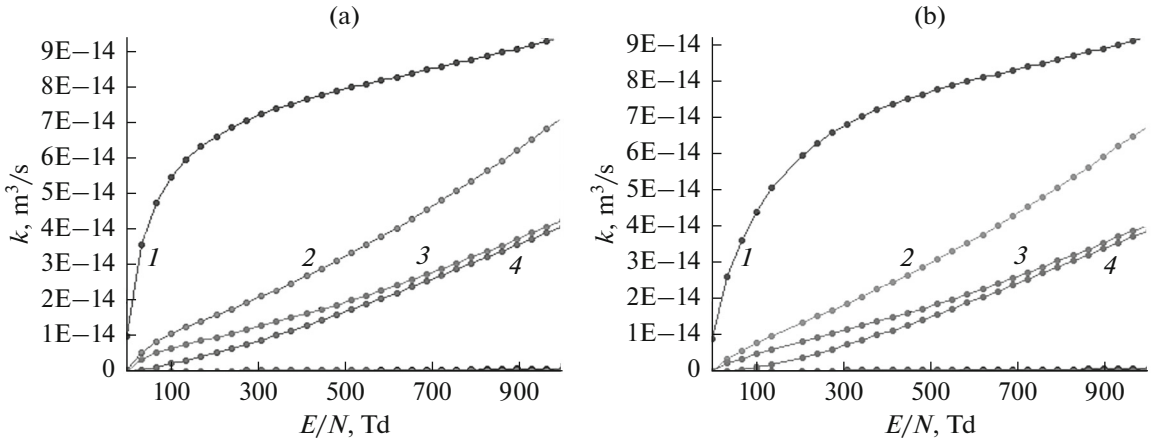

Fig. 9. Rate constants of electron collisions of electrons with silver atoms versus E/N in plasma of mixture of vapors Ag_2S and krypton 200–101 300 (a) and 1000–101 300 Pa (b): (*1*) elastic scattering of electrons on silver atoms, (*2*) excitation of atom state (E_{thr} = 3.78 eV), (*3*) excitation of state (E_{thr} = 3.66 eV), and (*4*) ionization of atoms (E_{thr} = 8.00 eV).

Figure 10 presents the characteristic spectrum of the Raman scattering of the semiconductor laser radiation with a generation wavelength of 785 nm. Probing the synthesized film by micro-Raman spectroscopy at this wavelength made it possible to obtain the most intense spectrum of the Raman scattering in comparison with probing at a wavelength of 532 and 632.8 nm. The laser beam probed the area of the film surface 1–2 mm in diameter. The average power of the laser that generated the radiation at this wavelength was 32 mW. The spectra of the Raman scattering were identified on the basis of works [18], [19]. Thin films were studied using a Renishaw InVia™ confocal Raman microscope (United Kingdom). The exposition time was 10 s.

The spectrum of the light Raman scattering of the resultant film (Fig. 10) was characterized by the bands in the ranges 100–300 cm^{-1} with the maximums at 230.4, ~1000, and 1302 cm^{-1}. The band in the range 210–250 cm^{-1}, including the maximum at 230.4 cm^{-1}, is caused by the Ag_2S nanoparticles, and they are due to the symmetrical longitudinal oscillatory modes of the Ag–S–Ag bonds [18]. A wide band in the range 1200–1300 cm^{-1} is associated with the oscillations of silver released at the photoinduced decomposition of Ag_2S. The observed wide band in the range 1500–1650 is also associated with the photo decomposition of Ag_2S [20].

Table 5. Constants of excitation rates of a number of spectral lines of silver atoms for values E/N in plasma in mixture of vapors Ag_2S and krypton: 200–101 400 and 1000–101 300 Pa

E/N, Td	Mixture: Ag_2S–Kr = 101 300 : 200 Pa					
306	Ag	λ, nm	328.06	338.28	405.54	424.06
		k, m^3/s	0.2098×10^{-13}	0.1267×10^{-13}	0.1683×10^{-16}	0.1658×10^{-17}
102	Ag	λ, nm	328.068	338.289	405.54	424.06
		k, m^3/s	0.1048×10^{-13}	0.6400×10^{-14}	0.5882×10^{-17}	0.1758×10^{-19}
E/N, Td	Mixture: Ag_2S–Kr = 101 300 : 1000 Pa					
304	Ag	λ, nm	328.068	338.289	405.54	424.06
		k, m^3/s	0.1873×10^{-19}	0.1133×10^{-13}	0.1447×10^{-16}	0.1255×10^{-17}
101	Ag	λ, nm	328.068	338.289	405.54	424.06
		k, m^3/s	0.7639×10^{-14}	0.4694×10^{-14}	0.3527E-17	0.5871×10^{-20}

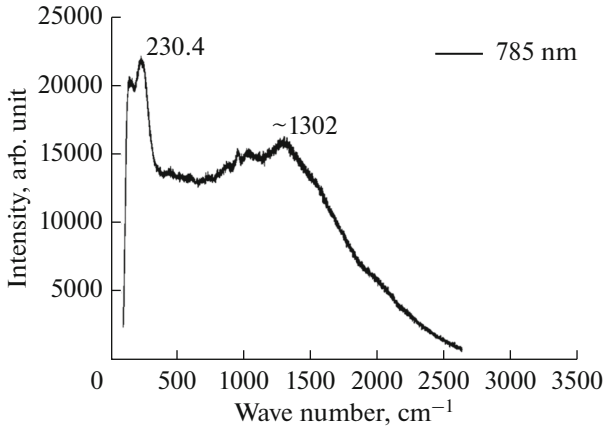

Fig. 10. Spectrum of Raman scattering of laser radiation at wavelength of 785 nm by a thin film synthesized from electrode erosion products of overvoltage nanosecond discharge between electrodes of Ag_2S SIC (p(Ar) = 101 kPa).

CONCLUSIONS

The investigation into the characteristics of the overvoltage nanosecond discharge in krypton between the electrodes of Ag_2S SIC revealed the following:

(i) at a distance between the electrodes of 2 mm, the space-homogeneous discharge was ignited whose form was determined by the energy contribution into plasma and the pulse repetition frequency;

(ii) the maximum voltage over the discharge gap was 27 kV at its total duration up to 450 ns, and the individual oscillations of the voltage pulse had a duration of 20–30 ns; the maximum amplitude of current pulses was 250 A and the value of the pulse electric power reached 10 MW at an individual pulse power of 631 mJ;

(iii) in the spectrum of the discharge plasma radiation, the radiation of the one-charge silver ions in the spectral range 200–300 nm and the silver atoms in the spectral range 300–340 prevailed, which is promising for the design of a point UV-lamp using the Ag_2S compound vapors;

(iv) the investigation into the synthesized surface structures based on Ag_2S, which is what the discharge electrodes are made of, showed that they are homogeneous enough.

The numerical simulation of plasma parameters in the mixture of the vapors of Ag_2S and krypton established that, for the range of E/N 306–101 Td of the experimental study of the electrical and optical characteristics of the discharge, the average energies of electrons varied in the range from 7.213 to 4.789 eV. Their highest energies correspond to the values 73.51–33.78 eV for the first mixture and 77.12–30.31 eV for the second mixture. The values of the electron concentration were for the mixture Kr–Ag_2S: 7.2×10^{19}–3.89×10^{20} cm^{-3} at 101 300 : 200 Pa and 7.2×10^{19}–3.6×10^{20} cm^{-3} at 101 300 : 1000 Pa.

The specific power of the discharge losses at the inelastic and elastic processes of the electron collisions with atoms and molecules in the composition of the working mixtures of the gas-discharge plasma was increased per unit of the total concentration of the mixture with the growth in the value of E/N both for the inelastic and elastic processes. Its maximum value was for the inelastic processes in the mixture of vapors Ag_2S and krypton 1000–103 000 Pa, and its value was 0.6220×10^{-13} eV m^3/s for E/N 306 Td.

The specific losses of discharge power in the mixtures Ag_2S– Kr = 200–101 300 Pa and Ag_2S–Kr = 1000–101 300 Pa in the inelastic processes of the collisions of electrons with silver atoms reached the value of 82% for the second mixture and 55% for the first mixture at E/N = 35 Td. For the mixture Ag_2S–Kr = 1000–101 300 Pa, they were higher than for the mixture Ag_2S– Kr = 200–101 300 Pa by about 2 times. In the case of excitation of the line of silver atoms with a wavelength λ = 328.068 nm at E/N = 1 Td, they made up 42%.

The constants of the excitation rates of spectral lines 328.068, 338.289, and 405.54 nm of silver atoms in the mixture Ag_2S– Kr = 200–101 300 Pa are in the limits $(0.5427–0.2132) \times 10^{-13}$ m^3/s, $(0.3247–0.1286) \times 10^{-13}$ m^3/s, $(0.5730–0.1789) \times 10^{-16}$ m^3/s, respectively. They had higher values than for the mixture with a high partial pressure of Ag_2S (1000 Pa). The rate constant of the spectral line excitation 424.06 nm of the silver ion is in the limits $(0.2535 \times 10^{-16}–0.2568 \times 10^{-17})$ m^3/s. The maximum value of the constant of the excitation rate of the resonant spectral line 328.068 nm of silver atoms was a value of (0.2098×10^{-13}) m^3/s for E/N 306 Td for the mixture of vapors of Ag_2S and krypton at the values of partial pressures 200 and 101 300 Pa, respectively.

The investigation into the Raman spectra of the thin films synthesized of plasma based on the krypton–silver sulphide gas–vapor mixture showed that they consisted of Ag_2S. This fact can be used to design various devices on the basis of the superionic conduction (supercapacitors, high capacity accumulators, and other electrical equipment).

CONFLICT OF INTEREST

The authors declare that they have no conflicts of interest.

REFERENCES

1. Tolstoguzov, A.B., Belykh, S.F., Gololobov, G.P., Gurov, V.S., et al., Ion-beam sources based on solid electrolytes for aerospace applications and ion-beam technologies (review), *Instrum. Exp. Techn.,* 2018, vol. 61, p. 159. https://doi.org/10.1134/S0020441218020100

2. Shuaibov, A.K., Minya, A.Y., Malinina, A.A., Malinin, A.N., et al., Study into synchronous flows of bactericidal ultraviolet radiation and transition oxides metals (Zn, Cu, Fe) in a pulsed gas discharge overvoltage reactor nanosecond discharge in the air, *Surf. Eng. Appl. Electrochem.,* 2020, vol. 56, no. 4, p. 510. https://doi.org/10.3103/S106837552004016X

3. Shuaibov, O.K., Minya, O.Y., Malinina, A.O., Malinin, O.M., et al., Electroluminescence of aluminium-oxides nanoparticles in overstressed nanosecond discharge plasma in high-pressure air, *Nanosistemy, Nanomaterialy, Nanotehnologii,* 2021, vol. 19, no. 1, p. 189.

4. Shuaibov, A.K., Minya, A.Y., Hrytsak, R.V., Malinina, A.A., et al., Characteristics of an overstressed discharge of nanosecond duration between electrodes of chalcopyrite in high pressure nitrogen, *Adv. Nanosci. Nanotechnol.,* 2020, vol. 4, no. 1, p. 1. https://doi.org/10.33140/ANN.04.01.01

5. Shuaibov, A.K., Minya, A.I., Malinina, A.A., Gritsak, R.V., et al., Characteristics and parameters of overstressed nanosecond discharge plasma in air between an electrode from aluminum and electrode from chalcopyrite ($CuInSe_2$), *Elektron. Obrab. Mater.,* 2021, vol. 57, no. 5, p. 34. https://doi.org/10.52577/eom.2021.57.5.34

6. Tominaga, K., Umezu, N., Mori, I., Ushiro, T., et al., Effects of UV light irradiation and excess Zn addition on ZnO:Al film properties in sputtering process, *Thin Solid Films,* 1998, vol. 316, p. 85. https://doi.org/10.1016/S0040-6090(98)00394-0

7. Mesyats, G.A., Ecton or electron avalanche from metal, *Phys.-Usp.,* 1995, vol. 165, no. 6, p. 601. https://doi.org/10.1070/PU1995v038n06ABEH000089

8. Shuaibov, O.K. and Malinina, A.O., Overstressed nanosecond discharge in the gases at atmospheric pressure and its application for the synthesis of nanostructures based on transition metals, *Progr. Phys. Metals,* 2021, vol. 22, no. 3, p. 382. https://doi.org/10.15407/ufm.22.03.382

9. Tarasenko, V.F., *Runaway Electrons Preionized Diffuse Discharge,* New York: Nova Science, 2014.

10. Striganov, A.R. and Sventitskii, N.S., *Tables of Spectral Lines of Neutral and Ionized Atoms,* New York: Springer, 1968. https://doi.org/10.1007/978-1-4757-6610-3

11. NIST Atomic Spectra Database Lines Form. https://physics.nist.gov/PhysRefData/ASD/lines_form.html.

12. Shuaibov, O.K., Gritsak, R.V., and Romanets', R.P., Emission characteristics of a nanosecond discharge plasma in air between electrodes from a superionic conductor (Ag2S), *The III Int. Scientific and Practical Conf. "Modern challenges to science and practice," Varna, Bulgaria,* January 24–26, 2022, p. 483.

13. BOLSIG+. Electron Boltzmann equation solver. http:/www.bolsig.laplace.univ-tlse.fr.

14. Smirnov, Yu.M., Electron-impact excitation of triplet levels of the zinc atom, *Opt. Spectrosc.,* 2008, vol. 104, no. 2, p. 159. https://doi.org/10.1134/S0030400X08020021

15. Dhanoj Gupta, Rahla Naghma, and Bobby Antony, Electron impact total and ionization cross sections for Sr, Y, Ru, Pd, and Ag atoms, *Can. J. Phys.,* 2013, vol. 91, no. 9, p. 744. https://doi.org/10.1139/cjp-2013-0174

16. Smirnov, Yu.M., Excitation of CuII and AgII in electron–atom collisions, *Quantum Electron.,* 1999, vol. 29, p. 1006. https://doi.org/10.1070/QE1999v029n11ABEH001624

17. Raizer, Yu.P., *Gas Discharge Physics,* Berlin: Springer-Verlag, 1991.

18. Malinina, A.O., Shuaibov, O.K., Malinin, O.M., and Bilak, Yu.Yu., Parameters of pulsed gas-discharge plasma based on gas-vapor mixture "krypton–silver sulfide," *Jubilee Conference "30 Years of the Institute of Electronic Physics of the National Academy of Sciences of Ukraine,"* Uzhhorod, September 21–23, 2022, p. 142.

19. Martina, I., Wiesinger, R., Jembrih-Simburger, D., and Schreiner, M., Micro-Raman characterisation of silver corrosion products: Instrumental set up and reference database, *e-PS,* 2012, vol. 9, p. 1.

20. Sadovnikov, S.I., Vovkotrub, E.G., and Rempel, A.A., Micro-Raman spectroscopy of nanostructured silver sulfide, *Dokl. Phys. Chem.,* 2018, vol. 480, p. 81. https://doi.org/10.1134/S0012501618060027

Translated by M. Myshkina